Journal of Hazardous Materials 416 (2021) 126182

Contents lists available at ScienceDirect

Journal of Hazardous Materials

journal homepage: www.elsevier.com/locate/jhazmat

Real-world particulate matters induce lung toxicity in rats fed with a high-fat diet: Evidence of histone modifications

Xuejingping Han [a,b,1], Meiping Tian [a,1], Pavel V. Shliaha [c], Jie Zhang [d,*], Shoufang Jiang [e], Bingru Nan [a,b], Md Nur Alam [a,b], Ole N. Jensen [c,*], Heqing Shen [d], Qingyu Huang [a,*]

[a] Key Laboratory of Urban Environment and Health, Institute of Urban Environment, Chinese Academy of Sciences, 1799 Jimei Road, Xiamen 361021, China
[b] University of Chinese Academy of Sciences, Beijing 100049, China
[c] Department of Biochemistry and Molecular Biology, VILLUM Center for Bioanalytical Sciences, University of Southern Denmark, Campusvej 55, DK-5230 Odense M, Denmark
[d] State Key Laboratory of Molecular Vaccinology and Molecular Diagnostics, School of Public Health, Xiamen University, 4221-117 Xiang An Nan Road, Xiamen 361102, China
[e] Department of Occupational and Environmental Health, School of Public Health, North China University of Science and Technology, Tangshan 063000, China

ARTICLE INFO

Editor: Dr. S Nan

Keywords:
Real-world PM exposure
High-fat diet
Histone modifications
DNA damage
Lung toxicity

ABSTRACT

Exposure to ambient particulate matters (PMs) has been associated with a variety of lung diseases, and high-fat diet (HFD) was reported to exacerbate PM-induced lung dysfunction. However, the underlying mechanisms for the combined effects of HFD and PM on lung functions remain poorly unraveled. By performing a comparative proteomic analysis, the current study investigated the global changes of histone post-translational modifications (PTMs) in rat lung exposed to long-term, real-world PMs. In result, after PM exposure the abundance of four individual histone PTMs (1 down-regulated and 3 up-regulated) and six combinatorial PTMs (1 down-regulated and 5 up-regulated) were significantly altered in HFD-fed rats while only one individual PTM was changed in rats with normal diet (ND) feeding. Histones H3K18ac, H4K8ac and H4K12ac were reported to be associated with DNA damage response, and we found that these PTMs were enhanced by PM in HFD-fed rats. Together with the elevated DNA damage levels in rat lungs following PM and HFD co-exposure, we demonstrate that PM exposure combined with HFD could induce lung injury through altering more histone modifications accompanied by DNA damage. Overall, these findings will augment our knowledge of the epigenetic mechanisms for pulmonary toxicity caused by ambient PM and HFD exposure.

1. Introduction

Air pollution caused by particulate matter (PM) is one of the most serious environmental problems worldwide. Extensive epidemiological studies have proved that exposure to PM, especially fine PM (PM2.5) is associated with a variety of adverse health outcomes, including pulmonary diseases (Zhou et al., 2020). Long-term exposure to ambient PM2.5 was found to be associated with the decreases in FVC, FEV1 and MMEF, which indicates a poorer lung function (Guo et al., 2019). It was shown that PM2.5 exposure is significantly related to the acute exacerbation of asthma and chronic obstructive pulmonary disease (COPD) in humans (Huang et al., 2018; Reid et al., 2019). In addition, the toxicological effects of PM2.5 on lung cells have been revealed by many animal and cell researches (Huang et al., 2014; Jiang et al., 2021). However, the potential molecular mechanisms of PM2.5-induced pulmonary injury remain largely unknown.

At present, the interactions between lifestyle and environmental factors actually play an important role in development of lung diseases. The adverse impacts of obesity on lung function have been widely acknowledged (Dixon and Peters, 2018; Littleton and Tulaimat, 2017), and the consumption of a high-fat diet (HFD) may be a risk factor for lung diseases by triggering dyslipidemia and obesity in human populations (Sacks et al., 2017). Epidemiological and experimental studies have demonstrated that obesity could aggravate the negative effects of airborne PM exposure on lung function. Kim et al. (2017) found that abdominal adiposity intensifies the inverse association of ambient air

* Corresponding authors.
E-mail addresses: jie.zhang@xmu.edu.cn (J. Zhang), jenseno@bmb.sdu.dk (O.N. Jensen), qyhuang@iue.ac.cn (Q. Huang).
[1] Authors contributed equally to this work.

https://doi.org/10.1016/j.jhazmat.2021.126182
Received 18 January 2021; Received in revised form 18 May 2021; Accepted 19 May 2021
Available online 23 May 2021

pollution with lung function in Korean men. Overweight and obesity was also associated with exacerbated responses to indoor PM exposure among individuals with asthma and COPD, suggesting that obese population are more susceptible to PM exposure (Lu et al., 2013; McCormack et al., 2015). Another study showed that long-term air pollution exposure was associated with lung function impairment, and the associations were stronger among obese and overweight than normal weight participants (Xing et al., 2020). Moreover, it was reported that the diesel exhaust particles (DEPs)-exposed obese rats had increased airway responses and inflammation compared to the nonobese rats, indicating the co-contribution of DEPs and obesity to asthma (Moon et al., 2014).

Nucleosome, the fundamental unit of chromatin, is composed of an octamer of four core histones (H2A, H2B, H3 and H4) wrapped with 147 base pairs of DNA. Histones are often subject to various post-translational modifications (PTMs) at their N-terminal "tails", including acetylation (ac), methylation (me), phosphorylation (ph), ubiquitination (ub), etc. As one of the most important epigenetic codes, histone modifications play pivotal roles in gene transcription, cell cycle, DNA damage repair, and cell fate determination (Kouzarides, 2007). The histone modification changes associated with PM exposure and lung injury have been documented, respectively (Li et al., 2017a). In addition, although there were limited reports on the epigenetic modifications (DNA methylation and miRNA) involved in PM-induced lung function impairment (Li et al., 2019, 2020), few studies payed attention to the role of histone PTMs (Bhargava et al., 2018). In a recent study, Ji et al. (2019) found that PM2.5 increased histone H3K27ac on gene promoters of *Stat2* and *Bcar1*, which contributed to lung dysfunction and inflammation in mice. PM2.5 exposure was also observed to exacerbate asthma in mice through enhancing H3K9 and H3K14 acetylation in *IL-4* gene promoter in $CD4^+$ T cells (Zhou et al., 2019). Furthermore, several studies showed that cigarette smoke increased phosphorylation of histone H3S10 and acetylation of H3K9 and H4K12, while diesel exhaust PM induced *COX-2* gene expression by regulating histone acetylation levels, which could result in lung inflammation, emphysema and tumor promotion (Rajendrasozhan et al., 2010; Ibuki et al., 2014; Cao et al., 2007). However, these work focused on only single or several specific histone marks, and the global response of lung histone PTMs to PM exposure was seldom figured out.

To date, most of the toxicological studies of PM usually use intratracheal instillation (IT) of PM extracts or inhalation of concentrated ambient PM as the exposure manners (Ying et al., 2015; Wang et al., 2017). The studies of exposure to real-world and non-concentrated PM, which is closer to real life, are still rarely carried out (Yan et al., 2014; Wei et al., 2016). In view of the evidence above, we hypothesized that HFD may aggravate real-world PM exposure-induced lung dysfunction through altering the pattern of histone PTMs. Therefore, by using a liquid chromatography tandem mass spectrometry (nanoLC/MS)-based proteomics approach, the current study aimed to compare the PM-induced histone PTM changes in lung between ND- and HFD-fed rats at a global level. In addition, the biological responses associated with histone PTM changes were also investigated. This study will provide novel insights into the epigenetic mechanism of lung toxicity induced by the combined exposure of PM and HFD, and aid us in better understanding the coactions of air pollution and lifestyle on respiratory health.

2. Materials and methods

2.1. Animals and real-world PM exposure

Forty Sprague-Dawley (SD) male rats (three-weeks old) were purchased from SLAC Laboratory Animal (Shanghai, China). All rats were maintained on animal chow with free access to pellet and water in plastic cages on standard conditions (21–22 °C room temperature, 40–60% relative humidity with a 12 h light/dark cycle) during the study period. After one week acclimation rats were randomly divided into four groups ($n = 10$ per group): (1) ND-control group fed with normal diet (ND) and treated with filtered air; (2) ND-PM group fed with ND and treated with PM; (3) HFD-control group fed with high-fat diet (HFD) and treated with filtered air; and (4) HFD-PM group fed with HFD and treated with PM. The caloric supply of HFD was 45.7% from lipids, 37.9% from carbohydrates and 16.5% from protein. PM-treated rats were exposed to continuous, non-concentrated, real-world PM through an individually ventilated caging (IVC) air-handling system (Tecniplast Inc., Exton, PA, USA), while the control rats were exposed to filtered air with the addition of a high-efficiency particulate air (HEPA) filter positioned in the inlet valve to remove all the PMs. The system was located at a laboratory in North China University of Science and Technology in Tangshan, a northern city in China. The exposure was performed 24 h/day and 7 days/week for a total of 6 months (from January 1, 2016 to June 30, 2016). The PM (PM1.0, PM2.5 and PM10) concentrations in rat cages were monitored by using a portable air quality detector. After exposure the rats were euthanized and lung tissues were dissected and stored at −80 °C for further analysis. The protocol for animal experiments were approved by the Research Ethics Committee of Institute of Urban Environment, Chinese Academy of Sciences.

2.2. Histone extraction and sample preparation for nanoLC-MS analysis

Lung histones were acid extracted as described previously with slight modifications (Tvardovskiy et al., 2015). In brief, 100 mg of lung tissue was homogenized in nuclear isolation buffer (NIB) containing 0.3% (v/v) NP-40, protease inhibitors and phosphatase inhibitor. The homogenate was then centrifuged at 1000 g for 5 min and the nuclear pellet was collected and washed with NIB without NP-40 for 2 times. Histones were extracted by incubation of the nuclear in 0.2 M H_2SO_4 for 1 h. After centrifugation at 14,000 g for 5 min, the supernatant (histone) was collected and purified by size exclusion chromatography (SEC) using PD MiniTrap™ columns (GE Healthcare, USA). The histone concentration was measured by BCA assay.

Histone was processed for nanoLC-MS analysis as reported previously (Maile et al., 2015). Ten microgram (10 μg) of histone sample was buffered to pH 8.5 by addition of 1 M triethylammonium bicarbonate and incubated with 1% (v/v) propionic anhydride in acetonitrile for 30 min at room temperature. The reaction was then quenched with 80 mM hydroxylamine (20 min at room temperature). Tryptic digestion was performed for overnight with 0.5 μg trypsin (Promega Sequencing Grade, USA) at 37 °C. After digestion, 1% (v/v) phenyl isocyanate in acetonitrile was added to each sample and incubated with shaking for 1 h at 37 °C. The samples were finally diluted with 1% trifluoroacetic acid (TFA) and 100 ng of tryptic peptides were loaded for nanoLC-MS analysis.

2.3. NanoLC-MS/MS analysis

The peptides were analyzed by using a nanoACQUITY UPLC system (Waters, Milford, MA, USA) coupled to an Orbitrap Velos Pro mass spectrometer (Thermo Fisher, USA). The samples were trapped on a Symmetry C18 column (5 μm, 180 μm × 20 mm i.d.) and desalted at 3 μL/min flow rate for 3 min with 0.1% TFA. The mobile phases were (A) 0.1% formic acid in water as aqueous phase and (B) 0.1% formic acid in acetonitrile as organic phase. The separation was performed on a HSS T3 column (1.8 μm, 75 μm × 250 mm i.d.) at 0.3 μL/min flow rate with the following gradient: 0 min, 2% B; 45 min, 35% B; 70 min, 60% B; 80 min, 80% B. The column temperature was maintained at 40 °C and the injection volume was 3 μL.

Runs were acquired using data independent acquisition (DIA) method (Sidoli et al., 2015). A full scan MS spectrum (m/z 300−1100) was acquired in the Orbitrap with a resolution of 120000 (at 200 m/z) followed by 16 MS/MS events spanning through the mass range, each acquired in the ion trap with an isolation window of 50 m/z. The automatic gain control (AGC) target was set to 5×10^5 in the Orbitrap or

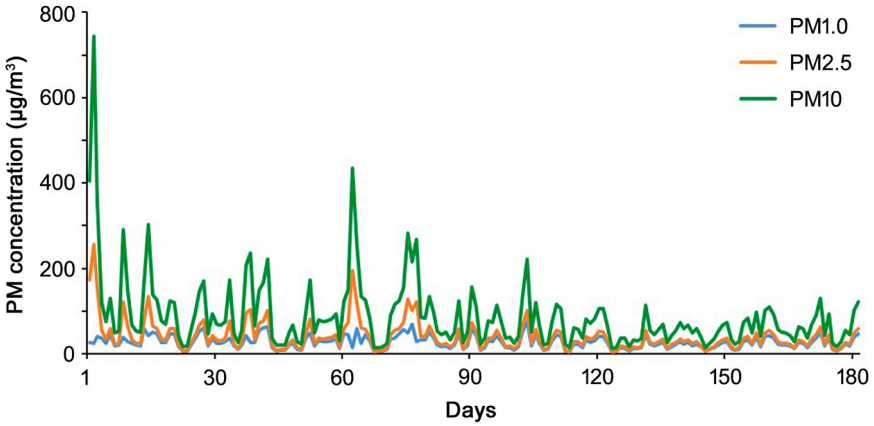

Fig. 1. Daily concentrations of PM1.0, PM2.5 and PM10 monitored over the entire exposure period.

3×10^4 in the ion trap. Fragmentation was performed using collision-induced dissociation (CID) set at 35%. MS/MS was performed with an AGC target of 3×10^4 using an injection time limit of 50 ms.

2.4. Data processing

The acquired LC-MS raw data were analyzed using EpiProfile 2.0 software for the identification and quantification of histone modifications (Yuan et al., 2018). The software was run on Matlab platform, and the parameters were set as follows: the organism was rat; the source was normal histone; and the subtype was set to "N14 light Mods". To quantify the level of a particular histone modification species, the relative abundance of a given peptide was calculated by dividing its area by the total area of that peptide in all of its modified forms (including unmodified form).

2.5. Western blotting

Lung histones (10 μg) or total proteins (50 μg) were separated by SDS-PAGE and transferred to polyvinylidene difluoride (PVDF) membranes. The membranes were blocked with 5% non-fat milk and then incubated with primary antibodies of anti-H3, anti-H4, anti-H3K4me2, anti-H3K18ac, anti-H3K23me1, anti-H4K8ac, anti-H4K12ac (1:2000 dilution; Abcam, USA), anti-β-Actin, anti-p53, anti-phosphorylated p53 (Ser15), anti-Chk1, anti-phosphorylated Chk1 (Ser345) and anti-γ-H2AX (1:2000 dilution; Cell Signaling Technology, USA) at 4 °C for overnight. The membranes were washed with TBST followed by 1 h incubation with HRP-conjugated goat anti-mouse IgG or anti-rabbit IgG secondary antibody (1:10000 dilution). The blots were developed by using an enhanced chemiluminescence (ECL) kit and then visualized on Kodak image station 4000MM (Carestream Health, INC). The intensity of protein bands was quantified by using Image J software (NIH, USA). The levels of modified histones were quantified relative to H3 signal, while levels of other target proteins were quantified relative to β-Actin level.

Table 1
Effects of PM exposure on body weight, lung weight and lung coefficient in rats.

Group		Body weight (BW, g)	Lung weight (LW, g)	Lung coefficient (LW/BW, %)
Normal diet (ND)	Control	704.78 ± 103.22	1.00 ± 0.30	0.14 ± 0.05
	PM exposure	654.90 ± 69.37	1.13 ± 0.29	0.18 ± 0.07
High-fat diet (HFD)	Control	820.68 ± 74.36	0.88 ± 0.09	0.11 ± 0.01
	PM exposure	750.48 ± 66.52*	1.00 ± 0.14*	0.13 ± 0.02**

Difference between control and PM exposure groups for HFD-fed rats,
* $p < 0.05$,
** $p < 0.01$.

2.6. DNA damage ELISA assay

DNA damage assay was performed using DNA oxidative damage ELISA kit according to the manufacturer's protocol (Cayman chemical, USA). Briefly, DNA was extracted from 10 mg of rat lung tissue, digested using nuclease P1 (Sigma), and incubated with alkaline phosphatase at 37 °C for 30 min. Fifty microliter of DNA samples (5 μg) and standards were added to the wells of the plate, and 50 μL DNA damage AChE Tracer and ELISA antibody were subsequently added to the wells. The plate was then covered with plastic film and incubated for 18 h at 4 °C. The liquids in the wells were removed and 200 μL Ellman's reagent was added. The plate was covered again with film and incubated in the dark at room temperature for 120 min with shaking. The plate was then read at a wavelength of 412 nm using a microplate reader. The concentration of damaged DNA was calculated according to the plotted standard curve.

2.7. Statistical analysis

All data were expressed as mean ± SD and subjected to statistical analysis by using the SPSS software (Version 19.0). Significant differences between two groups were determined by the *t*-test with equal variance. Two-way analysis of variance (ANOVA) followed by LSD post hoc test was used to analyze the main effects of PM exposure, diet, and their interaction (PM × diet). Data were graphically presented using the plots for two factors (PM × diet), where two parallel lines indicated no interactions while nonparallel lines with a *p*-value <0.05 indicated a significant interaction (Jiang et al., 2020). The Pearson correlations between histone PTMs, and between histones and DNA damage levels were analyzed by using the MetaboAnalyst software (http://www.metaboanalyst.ca/). $p < 0.05$ was considered statistically significant, and the false discovery rate (FDR) was applied to correct for multiple hypothesis tests.

3. Results and discussion

3.1. Effects of real-world PM exposure on rat body weight, lung weight and lung coefficient

In this study, the real-world PM exposure was mainly performed from winter to spring (from January to June), 2016. The daily concentrations of PM1.0, PM2.5 and PM10 in the rat cages were monitored, and the concentrations of the former three months are much higher than those of the latter three months (Fig. 1). As shown in Table S1, the rats were exposed to 26.95 ± 2.67, 41.03 ± 14.81 and 88.22 ± 41.49 μg/m^3 of PM1.0, PM2.5 and PM10 averaged over the entire study period,

Table 2
Regulated individual and combinatorial histone PTMs in rat lung exposed to real-world PM.

Histone PTMs	Normal diet (ND)				High-fat diet (HFD)			
	Control (C, %)	PM exposure (P, %)	Ratio (P/C)	*p* value[a]	Control (C, %)	PM exposure (P, %)	Ratio (P/C)	*p* value[a]
H3K4me2	0.65 ± 0.04	0.40 ± 0.07	**0.62***	**0.030**	0.75 ± 0.16	0.70 ± 0.03	0.93	0.732
H3K18ac	3.76 ± 0.14	4.24 ± 0.25	1.13	0.103	3.58 ± 0.15	4.34 ± 0.38	**1.21***	**0.049**
H3K23me1	0.52 ± 0.08	0.49 ± 0.09	0.94	0.698	3.44 ± 0.15	0.59 ± 0.06	**0.17* ***	**0.000**
H4K8ac	3.35 ± 0.15	3.70 ± 0.15	1.10	0.103	3.31 ± 0.11	4.20 ± 0.39	**1.27***	**0.048**
H4K12ac	4.60 ± 0.07	5.06 ± 0.09	1.10	0.020	3.69 ± 0.29	5.13 ± 0.30	**1.39***	**0.016**
H3K9acK14ac	0.31 ± 0.02	0.29 ± 0.02	0.94	0.503	0.27 ± 0.01	0.33 ± 0.02	**1.22***	**0.035**
H3K18acK23ac	1.39 ± 0.05	1.42 ± 0.17	1.02	0.778	1.24 ± 0.12	1.74 ± 0.06	**1.40* ***	**0.009**
H3K27me1K36me1	2.66 ± 0.03	2.45 ± 0.27	0.92	0.503	2.48 ± 0.02	3.14 ± 0.17	**1.27* ***	**0.009**
H3K27me3K36me2	4.58 ± 0.18	4.13 ± 0.43	0.9	0.503	5.94 ± 0.31	4.35 ± 0.21	**0.73* ***	**0.009**
H4K5acK16ac	0.35 ± 0.02	0.29 ± 0.05	0.83	0.503	0.10 ± 0.04	0.33 ± 0.03	**3.30* ***	**0.009**
H4K12acK16ac	1.91 ± 0.05	1.93 ± 0.05	1.01	0.778	1.44 ± 0.14	2.05 ± 0.17	**1.42***	**0.019**

[a] *p* value was corrected by FDR, * $p < 0.05$, * * $p < 0.01$.

respectively. However, the PM concentrations were below 5 μg/m^3 in the control groups (data not shown). Since Tangshan is a heavy industry city located in northern China, its air pollution is usually the heaviest in winter and spring due to heat supply and weather condition. The PM2.5 and PM10 concentration is much higher than the WHO air quality guideline 10 μg/m^3 (for PM2.5) and 20 μg/m^3 (for PM10), respectively (WHO, 2005).

During the whole exposure period, PM did not cause any rat mortality. In addition, for ND groups, the body weight (BW), lung weight (LW) and lung coefficient (LC) of rats were not significantly altered after PM exposure. While for HFD groups, the BW was significantly lowered while LW and LC were both increased ($p < 0.05$) in PM-exposed rats compared with the controls (Table 1), indicating an adverse effect of PM and HFD co-exposure on rat growth and lung development. However, no significant interactions between PM and HFD on BW (F=0.247, $p = 0.623$), LW ($F = 0.067$, $p = 0.797$) and LC ($F = 0.087$, $p = 0.770$) were found (Fig. S1). These results suggested that real PM exposure could cause lung lesion in HFD-fed rats, however, the effects were not synergistically induced by PM and HFD. The histopathological changes were often observed in PM-induced lung injuries (Li et al., 2017b; Wong et al., 2018), and the increased LW and LC may indicate the lung swelling in rats.

3.2. Profiles of histone PTMs in rat lung

A nanoLC/MS-based proteomics analysis was performed to profile the histone PTMs in rat lung of the four groups. By Epiprofile software analysis, a total of 93 PTMs exist on histones H1, H2A, H3, H4 and noncanonical variants were identified and quantified, with 14 on H1, 34 on H2A, 36 on H3 and 9 on H4. However, no quantifiable PTMs were found on H2B. The detected PTMs were mono-methylation (me1), di-methylation (me2), tri-methylation (me3) and acetylation (ac), mainly on the N-terminal regions of histone sequence (Table S2). Moreover, it has been shown that PTMs can co-occur in combinational patterns on

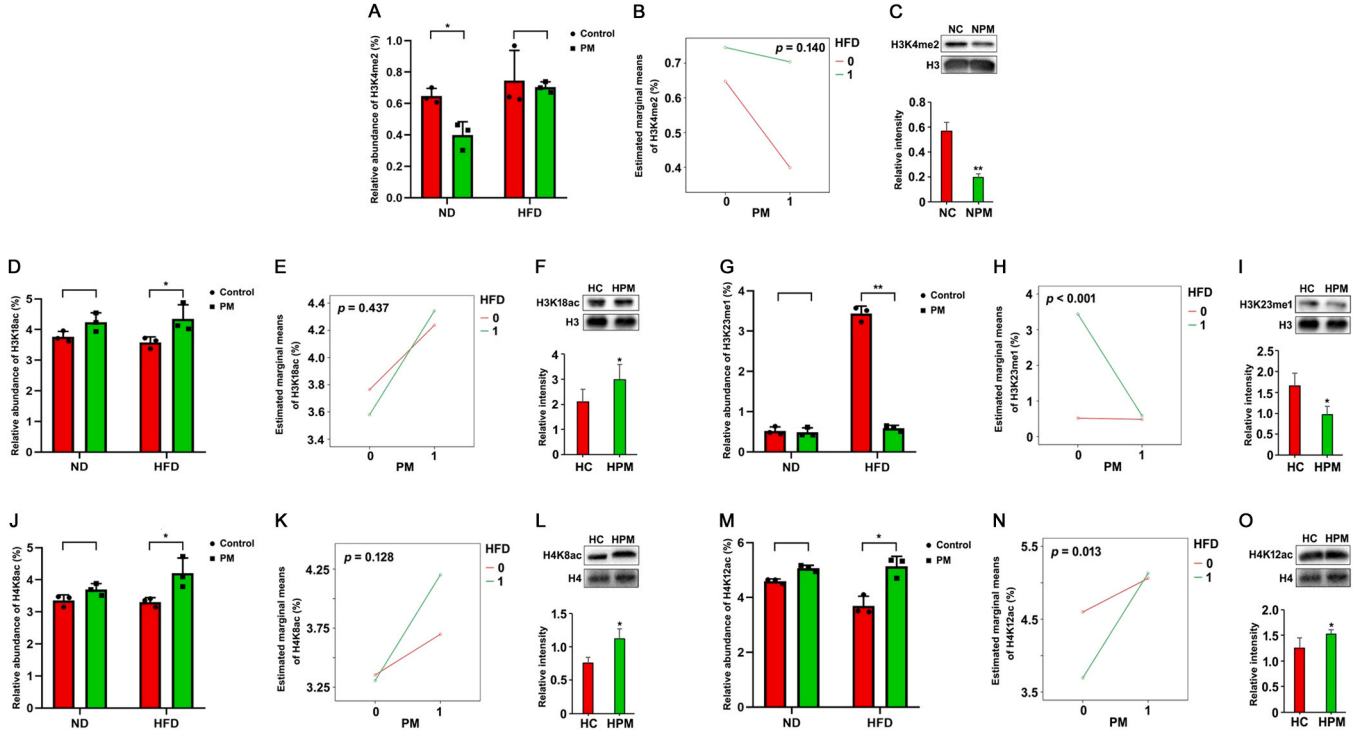

Fig. 2. Regulated individual histone PTMs in rat lungs following real-world PM exposure. (A, D, G, J, M) The relative abundance of H3K4me2, H3K18ac, H3K23me1, H4K8ac and H4K12ac in rat lungs. (B, E, H, K, N) Interaction between PM and HFD on H3K4me2, H3K18ac, H3K23me1, H4K8ac and H4K12ac. (C, F, I, L, O) The changes of histone PTMs were verified by Western blotting, and the levels of target histones were quantified relative to H3 or H4. Values were expressed as mean ± SD ($n = 3$), *$p < 0.05$, ** $p < 0.01$. NC, ND-control; NPM, ND-PM exposure; HC, HFD-control; HPM, HFD-PM exposure.

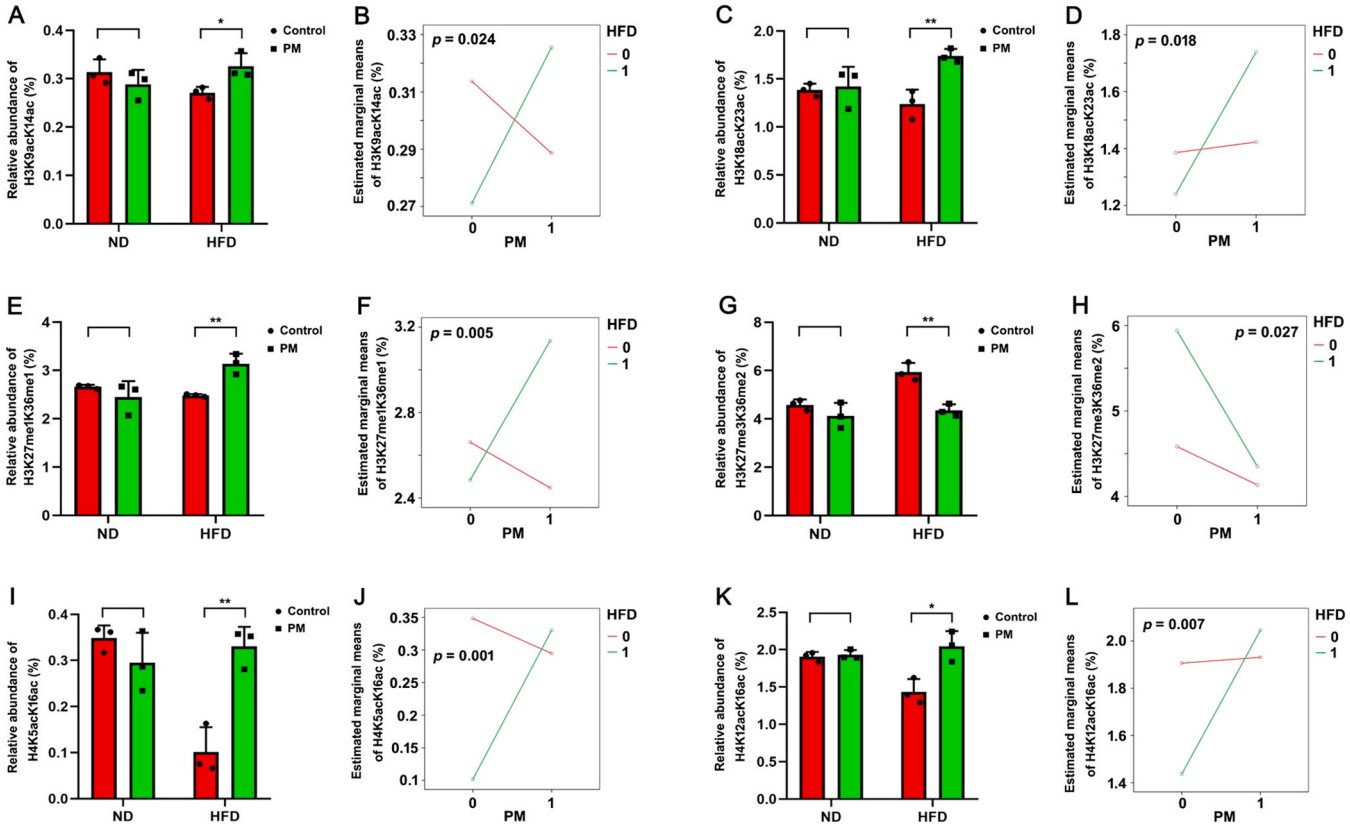

Fig. 3. Regulated combinatorial histone PTMs in rat lungs following real-world PM exposure. (A, C, E, G, I, K) The relative abundance of H3K9acK14ac, H3K18acK23ac, H3K27me1K36me1, H3K27me3K36me2, H4K5acK16ac and H4K12acK16ac in rat lungs. (B, D, F, H, J, L) Interaction between PM and HFD on H3K9acK14ac, H3K18acK23ac, H3K27me1K36me1, H3K27me3K36me2, H4K5acK16ac and H4K12acK16ac. Values were expressed as mean ± SD ($n = 3$), $^{*}p < 0.05$, $^{**}p < 0.01$.

the same peptide to form specific histone codes, the so called combinatorial PTMs (Tvardovskiy et al., 2017). In this study, we also detected 39 combinatorial PTMs with 8 on H2A, 20 on H3 and 11 on H4 (Table S2).

3.3. HFD and PM co-exposure altered more histone PTMs in rat lung

Since H3 and H4 are the two most important core histones, whose biological functions were widely studied, their regulations in response to PM exposure were mainly investigated in this work. To find out the differential histone PTMs in rat lung responsive to PM exposure, the relative abundance of both individual and combinatorial PTMs were compared between control and PM-exposed groups. To ensure the accuracy of PTM quantification, only the PTMs quantifiable in all the twelve samples (four groups with three replicates each) and with relative abundance ≥0.1% were selected for further analysis. As a result, among the retained 32 individual PTMs (Table S3), only one in ND groups while four in HFD groups showed significant expression differences ($p < 0.05$, ratio ≥1.2 or ≤0.8) in PM-exposed rats compared with the controls (Table 2 and Fig. S2). Specifically, only H3K4me2 was decreased in ND rats with PM exposure (Fig. 2A), and H3K23me1 were down-regulated (Fig. 2G) whereas H3K18ac, H4K8ac and H4K12ac were up-regulated by PM exposure in HFD rats (Fig. 2D, J and M). Moreover, the factorial analysis showed a significantly synergistic interaction between PM and HFD on H3K23me1 ($F = 389.099$, $p < 0.001$) and H4K12ac ($F = 10.156$, $p = 0.013$) (Fig. 2H and N) but not on H3K4me2 ($F = 2.680$, $p = 0.140$), H3K18ac ($F = 0.668$, $p = 0.437$) and H4K8ac ($F = 2.879$, $p = 0.128$) (Fig. 2B, E and K). These results indicated that although H3K23me1 and H4K12ac were not significantly changed by PM in ND rats, co-exposure to PM and HFD would synergistically regulating these two histone PTMs. To validate the MS results, the levels of the five changed individual PTMs were further analyzed by Western blotting. In good accordance with the MS results, H3K4me2 was decreased by PM in ND rats (Fig. 2C); H3K23me1 was decreased (Fig. 2I) while H3K18ac, H4K8ac and H4K12ac were increased in HFD rats with PM exposure (Fig. 2F, L and O), thus confirming the regulations of these PTMs in rat lung exposed to PM.

It is known that histones H3K4me2, H3K18ac, H4K8ac and H4K12ac are all associated with active transcription (Li et al., 2007). Cao et al. (2018) reported that lysine–specific demethylase 2 (LSD2) decreased *TFPI-2* expression by the demethylation of H3K4me2, thus contributing to the proliferation of small cell lung cancer (SCLC) cells. In contrast, KDM1A (also called LSD1) reduced H3K4me2 and repressed the transcription of *TIMP3*, which promoted non-small cell lung cancer (NSCLC) cell invasion (Kong et al., 2016). We found here that H3K4me2 was decreased in ND rat lung, which may indicate the carcinogenesis risk induced by PM exposure. Interestingly, H3K4me2 was not significantly changed by PM in HFD rats. Since HFD was prone to increase H3K4me2 in control rats (Table 2), it is speculated that HFD may have an antagonistic action against PM on H3K4me2, thereby attenuating the decrease of H3K4me2 induced by PM exposure. Additionally, the elevated H3K18ac and increased association of H3K18ac around the transcription start site of Δ*Np63*, *EGFR* and *STAT6* were observed in airway epithelial cells of asthmatic subjects (Stefanowicz et al., 2015). It was found that the up-regulation of H4K8ac and H4K12ac in human bronchial epithelial cells (BEAS-2B) account for the epithelial-mesenchymal transition (Liang et al., 2018). H4K12ac was also increased in the lung of smokers and COPD patients compared with nonsmokers (Sundar and Rahman, 2016). Therefore, the up-regulation of H3K18ac, H4K8ac and H4K12ac suggested that PM exposure may cause respiratory diseases in HFD-fed

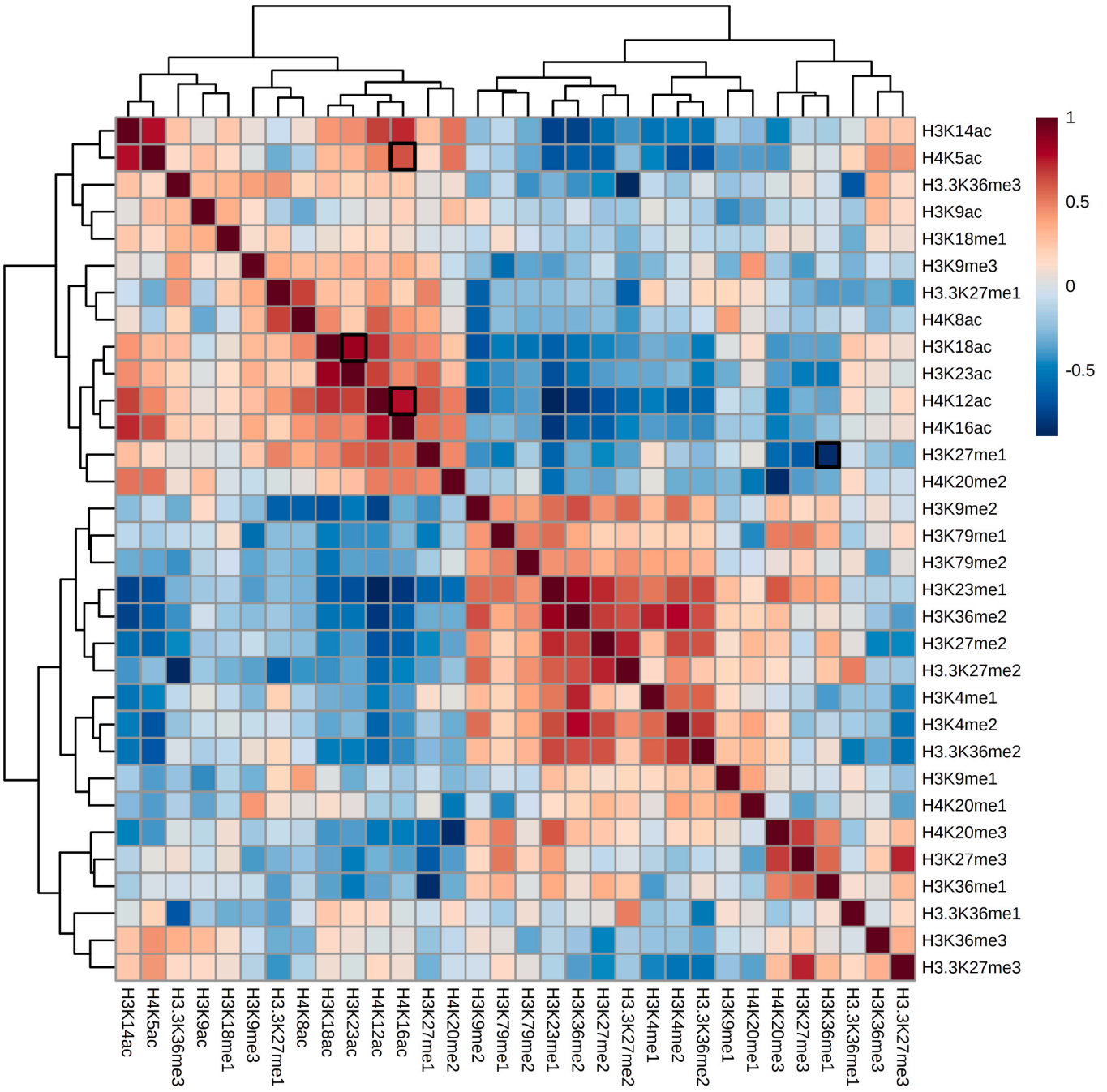

Fig. 4. Heat map of Pearson correlations between individual histone PTMs. Pairs with significant correlation ($p < 0.05$) are outlined by black boxes.

rats. In support of our findings, previous studies have pointed out that PM exposure altered various histone PTMs, which then resulted in lung dysfunction and tumor promotion (Ji et al., 2019; Zhou et al., 2019; Ibuki et al., 2014). Intriguingly, we also found a noncanonical histone PTM, H3K23me1 was remarkably depleted (5.89-folds) by PM in HFD group (Fig. 2G). Up to now, the biological functions associated with H3K23me1 are largely unclear, although it is known that H3K23me2 is related to transcriptional repression and H3K23me3 blocks DNA damage (Vandamme et al., 2015; Papazyan et al., 2014). In view of the significant interactions between PM and HFD, it is proposed that PM and HFD co-exposure synergistically altered H3K23me1 and H4K12ac, which may lead to lung dysfunction. However, the relationship between reduced H3K23me1 and lung toxicity still needs further studies.

Based on the screening criteria for differential individual PTMs, it was observed that among the 26 quantified combinatorial PTMs (Table S4), six in the HFD groups differentially expressed in rat lung after PM exposure while no significant changes were found for all the PTMs in ND groups (Table 2 and Fig. S3). The abundance of five PTMs H3K9acK14ac, H3K18acK23ac, H3K27me1K36me1, H4K5acK16ac and H4K12acK16ac were significantly elevated (Fig. 3A, C, E, I and K) while only H3K27me3K36me2 was lowered (Fig. 3G) by the combined exposure of PM and HFD. In addition, there was a significant interaction between PM and HFD on all the six combinatorial PTMs ($p < 0.05$) (Fig. 3B, D, F, H, J and L). Among them, PM and HFD have a synergistic interaction on H3K18acK23ac ($F = 8.716$, $p = 0.018$), H3K27me3K36me2 ($F = 7.342$, $p = 0.027$) and H4K12acK16ac ($F = 13.049$, $p = 0.007$) (Fig. 3D, H and L), suggesting that PM and HFD may affect lung function by co-regulating these histone PTMs.

The coexisting histone PTMs can affect the relative abundance of each other by attracting or repelling different histone modifying

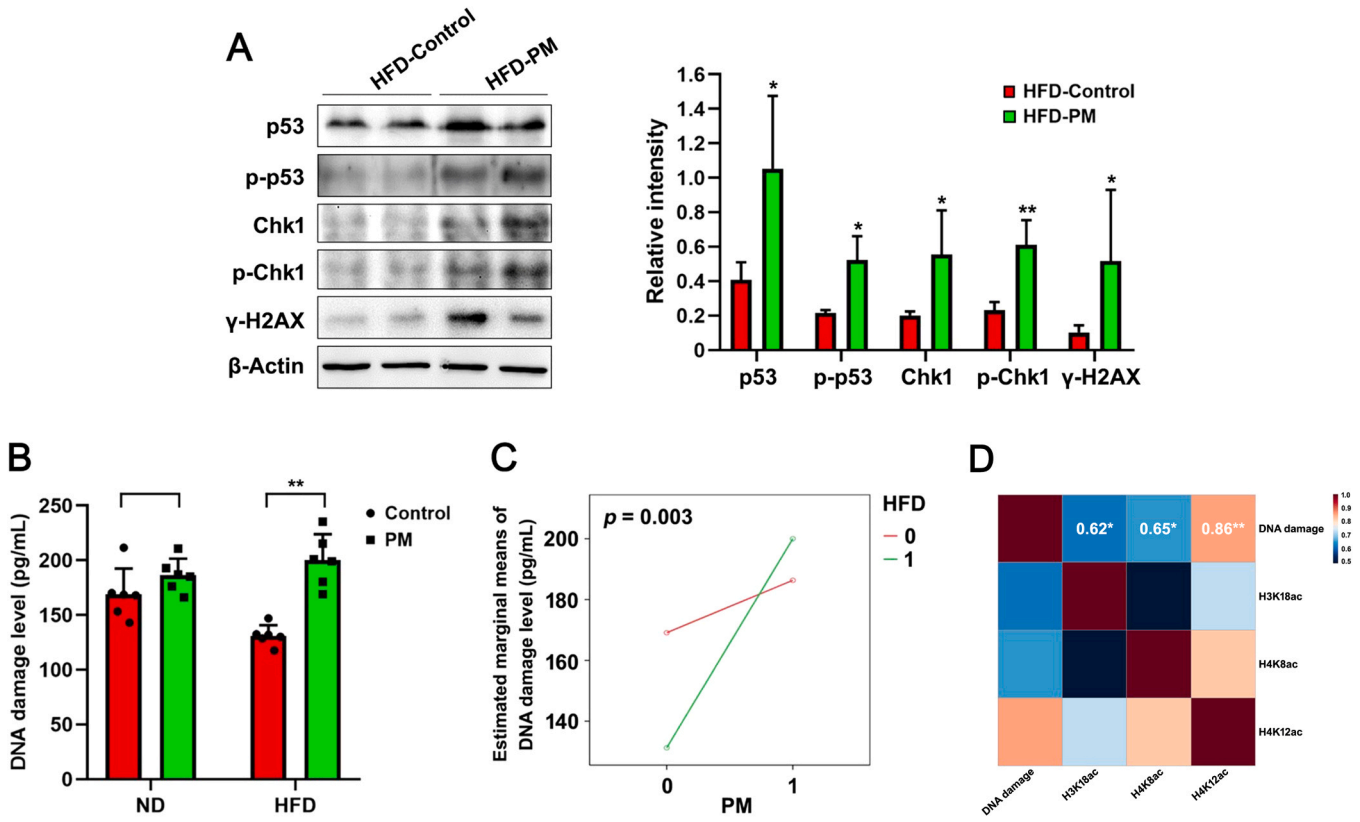

Fig. 5. Co-exposure of PM and HFD induced DNA damage in rat lung. (A) Western blot analysis of p53, p-p53, Chk1, p-Chk1 and γ-H2AX in lung of HFD-fed rats. The relative intensity of the target protein was normalized to β-Actin level. Values were expressed as mean ± SD ($n = 3$), $^{*}p < 0.05$, $^{**}p < 0.01$. (B) DNA damage levels in rat lungs. Values were expressed as mean ± SD ($n = 6$), $^{**}p < 0.01$. (C) Interaction between PM and HFD on DNA damage level. (D) Heat map of Pearson correlations between DNA damage and histone PTMs. $^{*}p < 0.05$, $^{**}p < 0.01$.

enzymes, generating a PTM crosstalk, which is emerging as an important regulatory mechanism for modulating chromatin states and transcriptional activity (Lee et al., 2010). It has been documented that H3K9ac, H3K14ac, H3K18ac, H3K23ac, H4K5ac, H4K12ac, H4K16ac and H3K36me1/2 are all associated with active gene expression while H3K27me1/3 is related to repressive gene expression. In addition, among the individual PTMs (Table S3), we observed significant positive correlations between H3K18ac and H3K23ac (r = 0.82), between H4K5ac and H4K16ac ($r = 0.61$) and between H4K12ac and H4K16ac ($r = 0.76$), however, H3K27me1 and H3K36me1 were negatively associated ($r = -0.84$) (Fig. 4 and Table S5), suggesting that H3K18ac and H3K23ac, H4K5ac and H4K16ac, and H4K12ac and H4K16ac exhibit a positive crosstalk while H3K27me1 and H3K36me1 have a negative crosstalk, and each two PTMs would have synergic effects when they coexisted (Tvardovskiy et al., 2017). H3K36 methylation was found to antagonize PRC2-mediated methylation of H3K27 (Yuan et al., 2011). Therefore, we propose that the combinatorial PTMs H3K27me1K36me1, H3K18acK23ac, H4K5acK16ac and H4K12acK16ac are all associated with active gene transcription, and the synergistically elevated H3K18acK23ac and H4K12acK16ac might contribute to lung toxicity in rats with combined exposure of PM and HFD. However, the interactions (not synergistic) on H3K27me1K36me1 and H4K5acK16ac need further elucidation. Consistent with our results, the up-regulations of H3K18ac, H3K23ac, H4K5ac, H4K12ac and H4K16ac were reported to promote the development of lung diseases (Stefanowicz et al., 2015; Hu et al., 2020; Liang et al., 2018; Chun et al., 2015). Taken together, based on the above results we found that PM exposure only altered one individual histone PTM in lung for ND rats while changed four individual and six combinatorial PTMs for HFD rats (Table 2). Moreover, the alterations of these PTMs are all associated with lung dysfunction, we thus suggest that together with HFD, PM may induce lung injury by modulating more histone modifications in rats.

3.4. Combined exposure of PM and HFD caused lung toxicity by inducing DNA damage

There are numerous studies suggest that histone modifications play vital roles in several chromatin-based processes, including DNA damage response. It has been demonstrated that H3K18ac, H4K8ac and H4K12ac are associated with DNA damage repair (Peterson and Laniel, 2004). Vazquez et al. (2016) reported that SIRT7 promotes DNA damage repair by H3K18 deacetylation at double-strand break (DSB) sites while DNA damaging agents increase H3K18ac level (Zhang et al., 2016). Besides, H4K8ac and H4K12ac are also recruited to DSBs for repair process when DNA damage occurred (Dhar et al., 2017). Interestingly, we observed the increase of H3K18ac, H4K8ac and H4K12ac in HFD-fed rats following PM exposure (Fig. 2), which may indicate the DNA damage in lungs. Moreover, many experimental data have revealed that PM2.5 exposure can induce DNA damage in lung cells (Wu et al., 2017; Yang et al., 2015; Li et al., 2017c). Therefore, we further investigated the DNA damage response of rat lung under PM stress. DNA damage triggers DNA repair process and results in accumulation of phosphorylated p53 (p-p53) and phosphorylated Chk1 (p-Chk1) to participate in DNA repair, and γ-H2AX is also a marker of DNA damage (Delia and Mizutani, 2017). As can be seen in Fig. 5A, the total p53, p-p53, total Chk1, p-Chk1 and γ-H2AX were all found to be significantly up-regulated in lung of HFD-fed rats with PM exposure, however, this was not observed in ND-fed rats (Fig. S4). In addition, the level of damaged DNA was found to be significantly elevated in HFD rats with PM exposure but not in ND rats (Fig. 5B), and the result also showed a synergistic interaction between PM and HFD on DNA damage ($F = 11.125$, $p = 0.003$) (Fig. 5C). These results suggested that DNA damage occurred in rat lung following

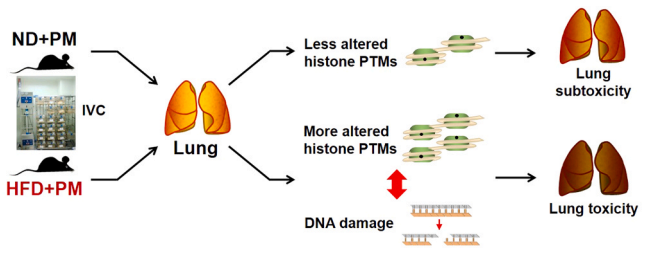

Fig. 6. Combined exposure of real-world PM and HFD induced lung toxicity through regulating more histone PTMs accompanied with DNA damage.

co-exposure of PM and HFD. Furthermore, it was shown that DNA damage level was positively correlated with H3K18ac ($r = 0.62$), H4K8ac ($r = 0.65$) and H4K12ac ($r = 0.86$) in HFD rats, respectively (Fig. 5D and Table S6), which confirmed the associations between DNA damage and these histone PTMs. Since H4K12ac was co-regulated by PM and HFD, it is proposed that PM exposure combined with HFD would cause lung injury by inducing DNA damage, which was especially involved in the enhanced H4K12ac.

4. Conclusion

In summary, by using a LC/MS-based proteomics approach, the present study comprehensively characterized the histone PTMs of rat lung for the first time. A set of individual and combinatorial PTMs were significantly altered in response to long-term, real-world PM exposure, which may contribute to lung dysfunction in rats. It was found that PM induced much more PTM changes in HFD than in ND rats, and co-exposure of HFD and PM may cause lung injury through synergistically regulating specific histone PTMs (H3K23me1, H4K12ac, H3K18acK23ac and H4K12acK16ac), accompanied by the activation of DNA damage response (Fig. 6). These findings could shed new light on the molecular mechanism of PM and HFD interaction-induced lung toxicity from an epigenetic aspect. Of note, since the real-world PM contains various PMs with different sizes and the exposure is thus a mixed one, it is difficult to determine the contribution of a specific PM to the lung histone modification changes. Moreover, further attentions should be payed to the functional characterization of combinatorial histone PTMs.

CRediT authorship contribution statement

Xuejingping Han: Methodology, Investigation, Data curation, Formal analysis, Writing - original draft. **Meiping Tian:** Investigation, Data curation, Validation, Writing - review & editing. **Pavel V. Shliaha:** Methodology, Data curation, Writing - review & editing. **Jie Zhang:** Conceptualization, Supervision, Validation, Project management. **Shoufang Jiang:** Methodology, Investigation. **Bingru Nan:** Investigation. **Md Nur Alam:** Investigation. **Ole N. Jensen:** Supervision, Validation, Writing - review & editing. **Heqing Shen:** Supervision, Validation. **Qingyu Huang:** Conceptualization, Funding acquisition, Supervision, Validation, Writing - review & editing.

Declaration of Competing Interest

The authors declare that they have no known competing financial interests or personal relationships that could have appeared to influence the work reported in this paper.

Acknowledgements

This work was financially supported by the National Natural Science Foundation of China (22076179, 21677142), the Natural Science Foundation of Fujian Province (2019J01138), the China Scholarship Council (20163035), the Xiamen Science and Technology Plan Project (3502Z20206091), the Youth Innovation Promotion Association of CAS (2019305), and the National Key R&D Program of China (2017YFC0211602, 2017YFC0211600). The VILLUM Center for Bioanalytical Sciences at SDU (Odense, Denmark) is supported by a generous grant from the VILLUM Foundation (Grant no. 7292 to O.N.J.). We thank Dr. Andrey Tvardovskiy (University of Southern Denmark) for help in the LC-MS analysis of histone PTMs and subsequent data analysis.

Appendix A. Supporting information

Supplementary data associated with this article can be found in the online version at doi:10.1016/j.jhazmat.2021.126182.

References

Bhargava, A., Bunkar, N., Aglawe, A., Pandey, K.C., Tiwari, R., Chaudhury, K., Goryacheva, I.Y., Mishra, P.K., 2018. Epigenetic biomarkers for risk assessment of particulate matter associated lung cancer. Curr. Drug Targets 19, 1127–1147.
Cao, D., Bromberg, P.A., Samet, J.M., 2007. COX-2 expression induced by diesel particles involves chromatin modification and degradation of HDAC1. Am. J. Respir. Cell Mol. Biol. 37, 232–239.
Cao, Y., Guo, C., Yin, Y., Li, X., Zhou, L., 2018. Lysine–specific demethylase 2 contributes to the proliferation of small cell lung cancer by regulating the expression of TFPI–2. Mol. Med. Rep. 18, 733–740.
Chun, S.M., Lee, J.Y., Choi, J., Lee, J.H., Hwang, J.J., Kim, C.S., Suh, Y.A., Jang, S.J., 2015. Epigenetic modulation with HDAC inhibitor CG200745 induces anti-proliferation in non-small cell lung cancer cells. PLoS One 10, 0119379.
Delia, D., Mizutani, S., 2017. The DNA damage response pathway in normal hematopoiesis and malignancies. Int. J. Hematol. 106, 328–334.
Dhar, S., Gursoy-Yuzugullu, O., Parasuram, R., Price, B.D., 2017. The tale of a tail: histone H4 acetylation and the repair of DNA breaks. Philos. Trans. R. Soc. Lond. B Biol. Sci. 372, 20160284.
Dixon, A.E., Peters, U., 2018. . The effect of obesity on lung function. Expert Rev. Respir. Med. 12, 755–767.
Guo, C., Hoek, G., Chang, L.Y., Bo, Y., Lin, C., Huang, B., Chan, T.C., Tam, T., Lau, A.K. H., Lao, X.Q., 2019. Long-term exposure to ambient fine particulate matter (PM2.5) and lung function in children, adolescents, and young adults: a longitudinal cohort study. Environ. Health Perspect. 127, 127008.
Hu, Q., Wang, C., Xiang, Q., Wang, R., Zhang, C., Zhang, M., Xue, X., Luo, G., Liu, X., Wu, X., Zhang, Y., Wu, D., Xu, Y., 2020. Discovery and optimization of novel N-benzyl-3,6-dimethylbenzo[d]isoxazol-5-amine derivatives as potent and selective TRIM24 bromodomain inhibitors with potential anti-cancer activities. Bioorg. Chem. 94, 103424.
Huang, Q., Hu, D., Wang, X., Chen, Y., Wu, Y., Pan, L., Li, H., Zhang, J., Deng, F., Guo, X., Shen, H., 2018. The modification of indoor PM2.5 exposure to chronic obstructive pulmonary disease in Chinese elderly people: a meet-in-metabolite analysis. Environ. Int. 121, 1243–1252.
Huang, Q., Zhang, J., Peng, S., Tian, M., Chen, J., Shen, H., 2014. Effects of water soluble PM2.5 extracts exposure on human lung epithelial cells (A549): a proteomic study. J. Appl. Toxicol. 34, 675–687.
Ibuki, Y., Toyooka, T., Zhao, X., Yoshida, I., 2014. Cigarette sidestream smoke induces histone H3 phosphorylation via JNK and PI3K/Akt pathways, leading to the expression of proto-oncogenes. Carcinogenesis 35, 1228–1237.
Ji, X., Yue, H., Ku, T., Zhang, Y., Yun, Y., Li, G., Sang, N., 2019. Histone modification in the lung injury and recovery of mice in response to $PM_{2.5}$ exposure. Chemosphere 220, 127–136.
Jiang, J., Li, Y., Liang, S., Sun, B., Shi, Y., Xu, Q., Zhang, J., Shen, H., Duan, J., Sun, Z., 2020. Combined exposure of fine particulate matter and high-fat diet aggravate the cardiac fibrosis in C57BL/6J mice. J. Hazard. Mater. 391, 122203.
Jiang, M., Li, D., Piao, J., Li, Y., Chen, L., Li, J., Yu, D., Pi, J., Zhang, R., Chen, R., Chen, W., Zheng, Y., 2021. Nrf2 modulated the restriction of lung function via impairment of intrinsic autophagy upon real-ambient PM2.5 exposure. J. Hazard. Mater. 408, 124903.
Kim, H.J., Park, J.H., Min, J.Y., Min, K.B., Seo, Y.S., Yun, J.M., Kwon, H., Kim, J.I., Cho, B., 2017. Abdominal adiposity intensifies the negative effects of ambient air pollution on lung function in Korean men. Int. J. Obes. 41, 1218–1223.
Kong, L., Zhang, P., Li, W., Yang, Y., Tian, Y., Wang, X., Chen, S., Yang, Y., Huang, T., Zhao, T., Tang, L., Su, B., Li, F., Liu, X.S., Zhang, F., 2016. KDM1A promotes tumor cell invasion by silencing TIMP3 in non-small cell lung cancer cells. Oncotarget 7, 27959–27974.
Kouzarides, T., 2007. Chromatin modifications and their function. Cell 128, 693–705.
Lee, J.S., Smith, E., Shilatifard, A., 2010. The language of histone crosstalk. Cell 142, 682–685.
Li, B., Carey, M., Workman, J.L., 2007. The role of chromatin during transcription. Cell 128, 707–719.
Li, J., Li, W.X., Bai, C., Song, Y., 2017a. Particulate matter-induced epigenetic changes and lung cancer. Clin. Respir. J. 11, 539–546.
Li, J., Wang, T., Wang, Y., Xu, M., Zhang, L., Li, X., Liu, Z., Gao, S., Jia, Q., Fan, Y., Wang, Z., Wu, N., Zhang, X., Dai, Y., Kong, F., Wang, W., Duan, H., 2020. Particulate

matter air pollution and the expression of microRNAs and pro-inflammatory genes: association and mediation among children in Jinan, China. J. Hazard. Mater. 389, 121843.
Li, R., Zhao, L., Tong, J., Yan, Y., Xu, C., 2017b. Fine particulate matter and sulfur dioxide coexposures induce rat lung pathological injury and inflammatory responses via TLR4/p38/NF-κB pathway. Int. J. Toxicol. 36, 165–173.
Li, R., Zhao, L., Zhang, L., Chen, M., Shi, J., Dong, C., Cai, Z., 2017c. Effects of ambient PM2.5 and 9-nitroanthracene on DNA damage and repair, oxidative stress and metabolic enzymes in the lungs of rats. Toxicol. Res. 6, 654–663.
Li, Z., Li, N., Guo, C., Li, X., Qian, Y., Yang, Y., Wei, Y., 2019. The global DNA and RNA methylation and their reversal in lung under different concentration exposure of ambient air particulate matter in mice. Ecotoxicol. Environ. Saf. 172, 396–402.
Liang, Z.L., Wu, D.D., Yao, Y., Yu, F.Y., Yang, L., Tan, H.W., Hylkema, M.N., Rots, M.G., Xu, Y.M., Lao, A.T.Y., 2018. Epiproteome profiling of cadmium-transformed human bronchial epithelial cells by quantitative histone post-translational modification-enzyme-linked immunosorbent assay. J. Appl. Toxicol. 38, 888–895.
Littleton, S.W., Tulaimat, A., 2017. The effects of obesity on lung volumes and oxygenation. Respir. Med. 124, 15–20.
Lu, K.D., Breysse, P.N., Diette, G.B., Curtin-Brosnan, J., Aloe, C., Williams, D.L., Peng, R. D., McCormack, M.C., Matsui, E.C., 2013. Being overweight increases susceptibility to indoor pollutants among urban children with asthma. J. Allergy Clin. Immunol. 131, 1017–1023.
Maile, T.M., Izrael-Tomasevic, A., Cheung, T., Guler, G.D., Tindell, C., Masselot, A., Liang, J., Zhao, F., Trojer, P., Classon, M., Arnott, D., 2015. Mass spectrometric quantification of histone post-translational modifications by a hybrid chemical labeling method. Mol. Cell. Proteom. 14, 1148–1158.
McCormack, M.C., Belli, A.J., Kaji, D.A., Matsui, E.C., Brigham, E.P., Peng, R.D., Sellers, C., Williams, D.L., Diette, G.B., Breysse, P.N., Hansel, N.N., 2015. Obesity as a susceptibility factor to indoor particulate matter health effects in COPD. Eur. Respir. J. 45, 1248–1257.
Moon, K.Y., Park, M.K., Leikauf, G.D., Park, C.S., Jang, A.S., 2014. Diesel exhaust particle-induced airway responses are augmented in obese rats. Int. J. Toxicol. 33, 21–28.
Papazyan, R., Voronina, E., Chapman, J.R., Luperchio, T.R., Gilbert, T.M., Meier, E., Mackintosh, S.G., Shabanowitz, J., Tackett, A.J., Reddy, K.L., Coyne, R.S., Hunt, D. F., Liu, Y., Taverna, S.D., 2014. Methylation of histone H3K23 blocks DNA damage in pericentric heterochromatin during meiosis. Elife 3, 02996.
Peterson, C.L., Laniel, M.A., 2004. Histones and histone modifications. Curr. Biol. 14, R546–R551.
Rajendrasozhan, S., Chung, S., Sundar, I.K., Yao, H., Rahman, I., 2010. Targeted disruption of NF-{kappa}B1 (p50) augments cigarette smoke-induced lung inflammation and emphysema in mice: a critical role of p50 in chromatin remodeling. Am. J. Physiol. Lung Cell. Mol. Physiol. 298, 197–209. L197-L209.
Reid, C.E., Considine, E.M., Watson, G.L., Telesca, D., Pfister, G.G., Jerrett, M., 2019. Associations between respiratory health and ozone and fine particulate matter during a wildfire event. Environ. Int. 129, 291–298.
Sacks, F.M., Lichtenstein, A.H., Wu, J.H.Y., Appel, L.J., Creager, M.A., Kris-Etherton, P. M., Miller, M., Rimm, E.B., Rudel, L.L., Robinson, J.G., Stone, N.J., Van Horn, L.V., 2017. Dietary fats and cardiovascular disease: a presidential advisory from the American heart association. Circulation 136, e1–e23.
Sidoli, S., Simithy, J., Karch, K.R., Kulej, K., Garcia, B.A., 2015. Low resolution data-independent acquisition in an LTQ-Orbitrap allows for simplified and fully untargeted analysis of histone modifications. Anal. Chem. 87, 11448–11454.
Stefanowicz, D., Lee, J.Y., Lee, K., Shaheen, F., Koo, H.K., Booth, S., Knight, D.A., Hackett, T.L., 2015. Elevated H3K18 acetylation in airway epithelial cells of asthmatic subjects. Respir. Res. 16, 95.
Sundar, I.K., Rahman, I., 2016. Gene expression profiling of epigenetic chromatin modification enzymes and histone marks by cigarette smoke: implications for COPD and lung cancer. Am. J. Physiol. Lung Cell. Mol. Physiol. 311, L1245–L1258.
Tvardovskiy, A., Schwämmle, V., Kempf, S.J., Rogowska-Wrzesinska, A., Jensen, O.N., 2017. Accumulation of histone variant H3.3 with age is associated with profound changes in the histone methylation landscape. Nucleic Acids Res. 45, 9272–9289.
Tvardovskiy, A., Wrzesinski, K., Sidoli, S., Fey, S.J., Rogowska-Wrzesinska, A., Jensen, O. N., 2015. Top-down and middle-down protein analysis reveals that intact and clipped human histones differ in post-translational modification patterns. Mol. Cell. Proteom. 14, 3142–3153.
Vandamme, J., Sidoli, S., Mariani, L., Friis, C., Christensen, J., Helin, K., Jensen, O.N., Salcini, E., 2015. H3K23me2 is a new heterochromatic mark in Caenorhabditis elegans. Nucleic Acids Res. 43, 9694–9710.
Vazquez, B.N., Thackray, J.K., Simonet, N.G., Kane-Goldsmith, N., Martinez-Redondo, P., Nguyen, T., Bunting, S., Vaquero, A., Tischfield, J.A., Serrano, L., 2016. SIRT7 promotes genome integrity and modulates non-homologous end joining DNA repair. EMBO J. 35, 1488–1503.
Wei, Y., Zhang, J.J., Li, Z., Gow, A., Chuang, K.F., Hu, M., Sun, Z., Zeng, L., Zhu, T., Jia, G., Li, X., Duarte, M., Tang, X., 2016. Chronic exposure to air pollution particles increases the risk of obesity and metabolic syndrome: findings from a natural experiment in Beijing. FASEB J. 30, 2115–2122.
WHO, 2005. Air quality guidelines–global update 2005. Available: ⟨https://www.euro.who.int/_data/assets/pdf_file/0005/78638/E90038.pdf⟩.
Wong, E.M., Walby, W.F., Wilsonm, D.W., Tablin, F., Schelegle, E.S., 2018. Ultrafine particulate matter combined with ozone exacerbates lung injury in mature adult rats with cardiovascular disease. Toxicol. Sci. 163, 140–151.
Wu, J., Shi, Y., Asweto, C.O., Lin, F., Yang, X., Zhang, Y., Hu, H., Duan, J., Sun, Z., 2017. Fine particle matters induce DNA damage and G2/M cell cycle arrest in human bronchial epithelial BEAS-2B cells. Environ. Sci. Pollut. Res. 24, 25071–25081.
Xing, X., Hu, L., Guo, Y., Bloom, M.S., Li, S., Chen, G., Yim, S.H.L., Gurram, N., Yang, M., Xiao, X., Xu, S., Wei, Q., Yu, H., Yang, B., Zeng, X., Chen, W., Hu, Q., Dong, G., 2020. Interactions between ambient air pollution and obesity on lung function in children: the Seven Northeastern Chinese Cities (SNEC) Study. Sci. Total Environ. 699, 134397.
Yan, Y.H., Chou, C.C.K., Wang, J.S., Tung, C.L., Li, Y.R., Lo, K., Cheng, T.J., 2014. Subchronic effects of inhaled ambient particulate matter on glucose homeostasis and target organ damage in a type 1 diabetic rat model. Toxicol. Appl. Pharmacol. 281, 211–220.
Yang, L., Wang, Y., Lin, Z., Zhou, X., Chen, T., He, H., Huang, H., Yang, T., Jiang, Y., Xu, W., Yao, W., Liu, T., Liu, G., 2015. Mitochondrial OGG1 protects against PM2.5-induced oxidative DNA damage in BEAS-2B cells. Exp. Mol. Pathol. 99, 365–373.
Ying, Z., Xie, X., Bai, Y., Chen, M., Wang, X., Zhang, X., Morishita, M., Sun, Q., Rajagopalan, S., 2015. Exposure to concentrated ambient particulate matter induces reversible increase of heart weight in spontaneously hypertensive rats. Part. Fibre Toxicol. 12, 15.
Yuan, W., Xu, M., Huang, C., Liu, N., Chen, S., Zhu, B., 2011. H3K36 methylation antagonizes PRC2-mediated H3K27 methylation. J. Biol. Chem. 286, 7983–7989.
Yuan, Z.F., Sidoli, S., Marchione, D.M., Simithy, J., Janssen, K.A., Szurgot, M.R., Garcia, B.A., 2018. EpiProfile 2.0: a computational platform for processing epi-proteomics mass spectrometry data. J. Proteome Res. 17, 2533–2541.
Zhang, P.Y., Li, G., Deng, Z.J., Liu, L.Y., Chen, L., Tang, J.Z., Wang, Y.Q., Cao, S.T., Fang, Y.X., Wen, F., Xu, Y., Chen, X., Shi, K.Q., Li, W.F., Xie, C., Tang, K.F., 2016. Dicer interacts with SIRT7 and regulates H3K18 deacetylation in response to DNA damaging agents. Nucleic Acids Res. 44, 3629–3642.
Zhou, J., Geng, F., Xu, J., Peng, L., Ye, X., Yang, D., Zhao, J., Sun, Q., 2019. $PM_{2.5}$ exposure and cold stress exacerbates asthma in mice by increasing histone acetylation in IL-4 gene promoter in $CD4^+$ T cells. Toxicol. Lett. 316, 147–153.
Zhou, Y., Ma, J., Wang, B., Liu, Y., Xiao, L., Ye, Z., Fan, L., Wang, D., Mu, G., Chen, W., 2020. Long-term effect of personal PM2.5 exposure on lung function: a panel study in China. J. Hazard. Mater. 393, 122457.